Chinese Chemical Letters 33 (2022) 3767–3771

Contents lists available at ScienceDirect

Chinese Chemical Letters

journal homepage: www.elsevier.com/locate/cclet

Integrated synthesis and ripening of $AgInS_2$ QDs in droplet microreactors: An update fluorescence regulating *via* suitable temperature combination

Ji Wang[1], Hao-Tian Ma[1], Liang-Jun Pan, Li Zhang, Zhi-Ling Zhang*

College of Chemistry and Molecular Sciences, Wuhan University, Wuhan 430072, China

ARTICLE INFO

Article history:
Received 17 July 2021
Revised 20 October 2021
Accepted 4 November 2021
Available online 11 November 2021

Keywords:
$AgInS_2$
Quantum dot
Ripening
Droplet microreactor
Temperature control

ABSTRACT

Aqueous phase synthesized ternary I–III–VI_2 Quantum dots (QDs) are getting more and more attention in biology researches, for their good biocompatibility and easy-to-adjust fluorescence properties. However, the quantum yield (QY) of these aqueous phase synthesized QDs are often pretty low, which seriously hindered their further applications in this field. In general, the ripening of the QDs helps to enhance their QY, closely related to the ripening temperature. But it is still hard to precisely control the fluorescence performance of the QDs products, due to the difficulties in precise temperature control and cumbersome temperature adjusting operations in batch reactors. Here we proposed an integrated droplet microfluidic chip for the automated and successive $AgInS_2$ QDs synthesis and ripening, with both temperatures controlled independently, precisely but easily. Taking advantage of the space-time transformation of the droplet microfluidic chips, the suitable temperature combination for $AgInS_2$ QDs synthesis and ripening was studied, and the high-performance $AgInS_2$ QDs were obtained. In addition, the reason for the decrease of QY of $AgInS_2$ QDs at higher ripening temperature was also explored.

$AgInS_2$ Quantum dots (QDs) are good representations of ternary I–III–VI_2 QDs, and with their easy-to-adjust fluorescence properties and good biocompatibility, they have been widely used as biosensors [1,2], in optical imaging [3–5] and in drug delivery [6]. Many methods have been reported for $AgInS_2$ QDs synthesis, among which the aqueous phase synthesis is most commonly used when the $AgInS_2$ QDs were synthesized for biological applications [7,8]. However, the quantum yield of the single-nucleus $AgInS_2$ QDs synthesized by this way is usually unsatisfying [9], making it difficult to meet the practical application requirements.

Though the quantum yield can be improved after the ripening of the QDs, compared with the synthesis process, the ripening process often requires a different reaction temperature, making the whole procedure labor-intensive when conducted in the traditional way [10]. Furthermore, like what the synthesis temperature does, the ripening temperature also affects the properties of the nanoparticles, and the synthesis efficiency could be critically reduced if the ripening temperature is not appropriately regulated [11]. Because that the change and regulation of the reaction condition is not easy in traditional batch reactors, there are still difficulties in both the study of how ripening temperature affects QDs' fluorescence properties and the precise control of QDs' performance. Therefore, a simple but flexible method to precisely regulate the reaction condition is in desperate need.

In recent years, droplet microreactors have shown outstanding advantages in the synthesis of many nanomaterials, including semiconductors [12] and amorphous nanomaterials [13,14]. This is because the efficient regulation and precise control of the synthesis conditions, which are based on the fast mass/heat transfer within these droplet microreactors [15,16]. Besides, benefit from the high-integration of microfluidic chips, droplet microreactors have been no longer confined to the only synthesis of nanomaterials, but become versatile when different functional units were integrated. When different reaction regions and on-line detecting units were integrated into a microfluidic chip, researchers can regulate the synthesis process and monitor the performance of the QDs in situ, so that the fluorescence properties can be adjusted on-line. Then, the research of QDs' performance regulation can be conducted and high-performance quantum QDs are obtained [17–19]. Baek *et al.,* for example, proposed a microfluidic platform integrated with mixing, aging and sequential growth regimes to study the decisive experimental parameters in InP nanocrystal synthesis [20]. Without

* Corresponding author.
E-mail address: zlzhang@whu.edu.cn (Z.-L. Zhang).
[1] These authors contributed equally to this work.

https://doi.org/10.1016/j.cclet.2021.11.022
1001-8417/

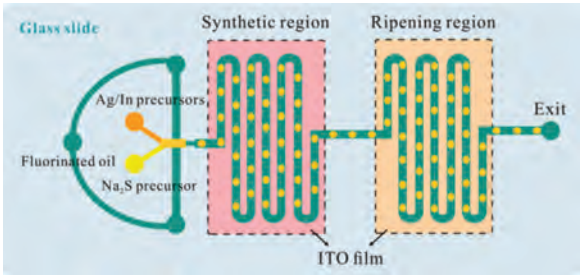

Fig. 1. Schematic diagram of the "synthesis-ripening" droplet microfluidic chip.

any intermediate purifications, Yashina *et al.* successfully synthesized core-shell $CuInS_2/ZnS$ QDs, with fluorescence spectrum ranging from 580 nm to 760 nm and high quantum yield, in two-stage droplet microreactors [21].

In this work, in order to study the effect of ripening temperature on QDs' performance, and to get high-performance water-soluble $AgInS_2$ QDs [22], an integrated droplet microfluidic chip was designed. Based on the unique space-time transformation characteristics of droplet microfluidic chips, two different regions to conduct QDs' synthesis and ripening were sequentially integrated into a droplet microfluidic chip, as shown in Fig. 1, with their temperature controlled independently by two temperature controllers. The overall height of the microchannel is 60 μm, and the widths of the main channel and the flow focusing neck are 100 μm and 50 μm, respectively. The number of channels in the synthesis region is 20, which is the same as that in the ripening region. As described before [22], the whole microfluidic chip was fabricated via soft lithography, and a portable fiber optic spectrometer (QE65000, Ocean Optics, USA) connected with an inverted fluorescence microscope (TE2000-U, Nikon, Japan) was employed again as the on-line fluorescence detector.

Apart from using fluorinated oil as the continuous phase, the composition of the reaction precursors in the dispersed phases (aqueous phase) were also the same with those in our previous work [22]. They are a solution containing 5 mmol/L Na_2S precursor and a mixture solution of Ag/In precursors and 3-mercaptopropionic acid (MPA, as QDs surface ligand). Besides, the injection rates of the fluorinated oil (40 μL/h) and the two precursor solutions (10 μL/h for each) also remained the same. After the mixing of the two precursor solutions, the original continuous water phase was divided into water-in-oil (W/O) droplets by the oil phase at the flow focusing port upstream of the chip, and then flow through the synthesis region, where the reaction begun to synthesize $AgInS_2$ QDs. After that, these droplets continued flowing to the next region, and the ripening was conducted. In this process, we altered the temperatures in both synthesis and ripening regions at 30, 50 and 70 °C respectively to study the effect of reaction temperature on the fluorescence properties of $AgInS_2$ QDs, with the help of the on-line fluorescence detector. All the synthesis-ripening temperature combinations are listed in Table S1 (Supporting information).

The stability of the microdroplets was observed to evaluate whether they are suitable for the continuous QDs' synthesis and ripening. As shown in Fig. S1a (Supporting information), droplets are formed steadily at the flow focusing point, and they remained stable as they flowed through the entire synthesis region (data not shown). Because that different temperatures are required in the synthesis and the ripening of $AgInS_2$ QDs, it is necessary to investigate the droplet stability when they flow through the synthesis region to the ripening region, where there would be a drastic change of their ambient temperature. Figs. S1b–d (Supporting information), show the stability of droplets when they entered the ripening region at different temperatures after they pass through the synthesis region at 50 °C. When the temperature of the ripening region varies from 30 °C to 70 °C, the droplets maintained stable and would not fuse with each other. The stability of the droplets flowing from a synthesis region at 30 °C to the ripening region at 70 °C was also evaluated and these droplets still remained good stability (data not shown) under this extreme temperature condition. It demonstrated that these droplet microreactors were suitable for the on-line continuous synthesis and ripening of $AgInS_2$ QDs.

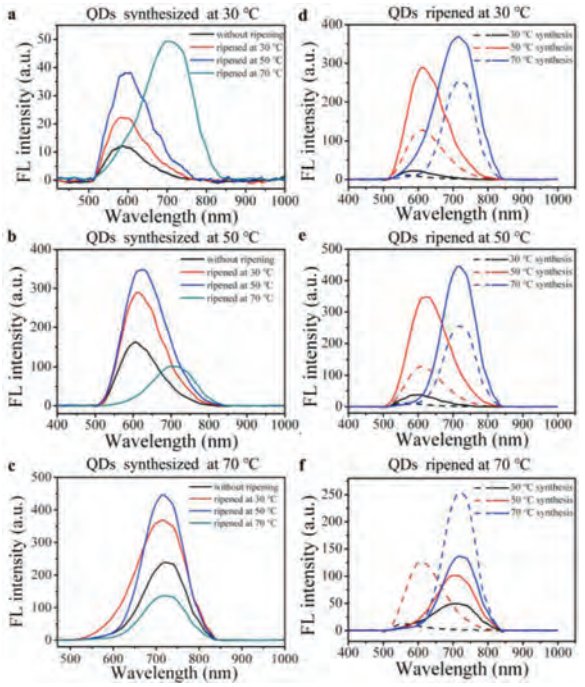

Fig. 2. (a–c) Fluorescence spectra of $AgInS_2$ QDs synthesized at (a) 30 °C, (b) 50 °C and (c) 70 °C before (black line) and after ripening at different temperatures (red line: 30 °C, blue line: 50 °C, and green line: 70 °C). (d-f) Fluorescence spectra of $AgInS_2$ QDs before and after ripened at (d) 30 °C, (e) 50 °C and (f) 70 °C. (The spectra of QDs without ripening are shown in dotted lines, spectra of QDs after the ripening at corresponding temperatures are shown in solid lines.).

The fluorescence signals of the QDs before and after ripening were collected online at the exits of the synthesis region and ripening region by a portable optical fiber spectrometer (QE65000, Ocean Optics, USA). QDs products before and after ripening were collected into a centrifugal tube through a bended glass capillary, also at the corresponding exits. All the products were prepared from same reactants at the same initial concentrations, and all the signals were collected under this same condition. These products were centrifuged at 10,000 rpm for 3 min, so that the products could be separated from the oil phase. After that, the products in the lower water phase were precipitated with ethanol, and centrifuged again at 6000 rpm for 3 min. The pure $AgInS_2$ QDs could be obtained by repeating the process above for 2 to 3 times for subsequent XRD, TEM and HRTEM characterization.

Fluorescence properties of $AgInS_2$ QDs synthesized at a same temperature but ripened at different temperatures were compared to evaluate the effect of ripening temperature on QDs' fluorescence properties. For the QDs synthesized at 30 °C (Fig. 2a), the fluorescence intensity (FI) increased from 12 a.u. to 22, 38 and 49 a.u. after the ripening at 30, 50 and 70 °C, respectively. The higher the ripening temperature was, the more the FI value increased. Besides, the fluorescence peak position red-shifted from 586 nm to 587 nm, 605 nm and about 720 nm after the ripening at 30 °C, 50 °C and 70 °C, respectively. This red-shift is because that at

30 °C, the reaction system could not provide enough energy for all precursors to complete the synthesis, so synthetic reaction went on at higher temperatures in the ripening region [22].

The maximum emission wavelength of the $AgInS_2$ QDs synthesized at 50 °C is about 606 nm, with an intensity of 161 a.u. (Fig. 2b). After the ripening at 30 °C, there came a significant FI increase to 290 a.u., without obvious peak shift. With the ripening temperature increased to 50 °C, the FI increased to 348 a.u., and the peak position red-shifted slightly to 627 nm. However, the FI decreased to 101 a.u., with the emission wavelength red-shifted to about 720 nm after the ripening at 70 °C. When synthesized at 70 °C, the position of the QDs' fluorescence peak maintained around 720 nm and would not be affected by the ripening temperature (Fig. 2c). The FI increased from 238 a.u. to 369 a.u. and 446 a.u., when the ripening temperature was 30 °C and 50 °C, respectively. But it decreased to 137 a.u. when the ripening temperature was 70 °C.

These results demonstrated that different ripening temperatures led to the change of the fluorescence performance, including emission peak position and the FI, of the final $AgInS_2$ QDs products. Therefore, to further figure out how the ripening temperature affect these fluorescence performance of the final products, emission peak position and the FI of the $AgInS_2$ QDs synthesized at different temperatures but ripened at a same temperature were also compared.

As shown in Fig. 2d, after ripened at 30 °C, the FI of QDs synthesized at all the set temperatures increased. And only QDs synthesized at 30 °C got a slightly red-shifted peak position because of the incomplete reaction in the synthesis region [22]. While the peak positions of QDs synthesized at 50 °C and 70 °C remained untouched. When the ripenings were conducted at 50 °C (Fig. 2e), the FI of all the QDs increased too, with the peak positions of QDs synthesized at 30 °C and 50 °C red-shifted. Only the peak positions of QDs synthesized at 70 °C did not change. When the ripening temperature reached to 70 °C (Fig. 2f), the fluorescence peaks of both the QDs synthesized at 30 °C and 50 °C red-shifted to about 720 nm after the ripening. But the fluorescence intensities of all the QDs, except those synthesized at 30 °C, decreased.

All these results showed that when the ripening temperature of $AgInS_2$ QDs was below the synthesis temperature, the fluorescence peak position of the QDs products remained unchanged. When $AgInS_2$ QDs were ripened at the same temperature as that of synthesis process, the fluorescence peak red-shifted slightly. When the ripening temperature was higher than the synthesis temperature, the fluorescence peak position red-shifted to the same position as the QDs synthesized at the higher temperature. That is, the emission peak position of the $AgInS_2$ QDs products were only determined by the higher temperature in the synthesis and ripening process. This is because that the free energy barrier of QDs is determined by the system temperature. And the higher temperature in the synthesis and ripening processes would determine the free energy barrier of the final QDs products, together with the size and the fluorescence peak position of QDs products [11].

However, though the emission peak position remained the same, the FIs of the QDs products prepared at the same synthesis-ripening temperature values but different temperature combination orders showed significant differences. We compared the fluorescence performance of two groups of $AgInS_2$ QDs as blow, to evaluate the exact role of temperature in synthesis and ripening process respectively. As shown in Fig. 3a, the fluorescence peak position of $AgInS_2$ QDs synthesized at 30 °C and ripened at 50 °C ($AgInS_2$–30–50) (605 nm), was nearly the same with that of QDs synthesized at 50 °C and ripened at 30 °C ($AgInS_2$–50–30) (606 nm), but the FI of $AgInS_2$–50–30 (290 a.u.) was higher than that of $AgInS_2$–30–50 (38 a.u.). And it was not a unique instance, but had its counterpart. As Fig. 3b shows, the fluorescence peak

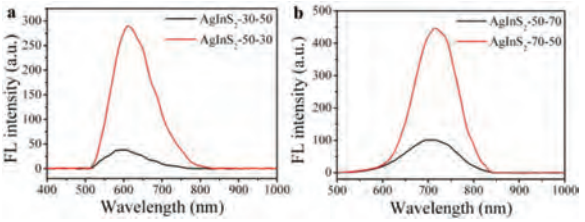

Fig. 3. Two groups of spectrum comparison of $AgInS_2$ QDs with opposite synthesis and ripening temperatures. (a) Spectrums of $AgInS_2$–30–50 and $AgInS_2$–50–30. (b) Spectrums of $AgInS_2$–50–70 and $AgInS_2$–70–50.

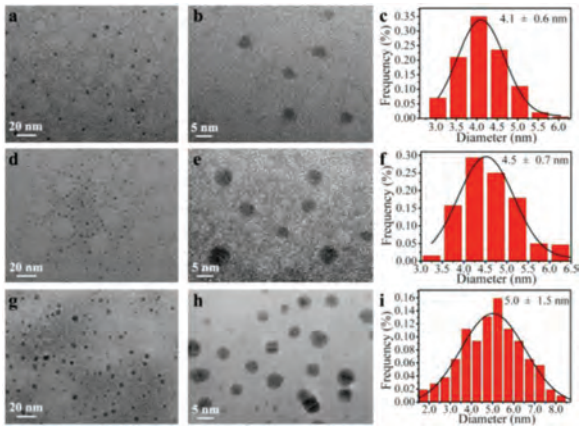

Fig. 4. TEM images, high-resolution TEM images and corresponding size distribution histograms of $AgInS_2$ QDs ripened at different temperatures. (a–c) 30 °C, (d–f) 50 °C, (g–i) 70 °C.

position of QDs synthesized at 50 °C and ripened at 70 °C ($AgInS_2$–50–70) (720 nm) was also the same with that of QDs synthesized at 70 °C and ripened at 50 °C ($AgInS_2$–70–50) (720 nm), and the FI of $AgInS_2$–70–50 (446 a.u.) was also much higher than that of $AgInS_2$–50–70 (101 a.u.). This phenomenon showed that, in the fluorescence performance regulation, not only the temperature values but also the combination order of the synthesis and ripening temperature matters.

The surface free energy barrier of QDs is formed by the competition between surface free energy and volume free energy, which is affected by system temperature and would determine the particle size of QDs products [11]. When the ripening temperature was lower than synthesis temperature, the energy provided by the ripening system was better for the growth of QDs, and there would be no obvious QDs aggregation, so the FI increased. When the ripening temperature was higher, Ostwald ripening would prevail in a short time, which led to a continuous aggregation of QDs particles, resulting in a broad size distribution range of QDs products, so the FI decreased [11,23]. Therefore, a suitable combination of synthesis-ripening temperature is in need to obtain high-performance water-soluble $AgInS_2$ QDs with a specific emission peak. Our present work showed that it was better to adjust the peak position through regulating the synthesis temperature. And the following ripening at a lower temperature than that of the synthesis process was conducive to the improvement of QDs' FI.

In order to figure out why the lower ripening temperatures helped to increase the FI of the QDs products, but the higher ripening temperature (70 °C) decreased QDs' FIs, $AgInS_2$ QDs synthesized at 50 °C before and after the ripening at 30, 50 and 70 °C were collected and observed by Field Emission Transmission Electron Microscopy (TEM, JEM2010, JEOL, Japan). As shown in Fig. 4, after ripening, the average particle size of $AgInS_2$ QDs increased from 4.0 ± 0.6 nm (Fig. S2 in Supporting information) to

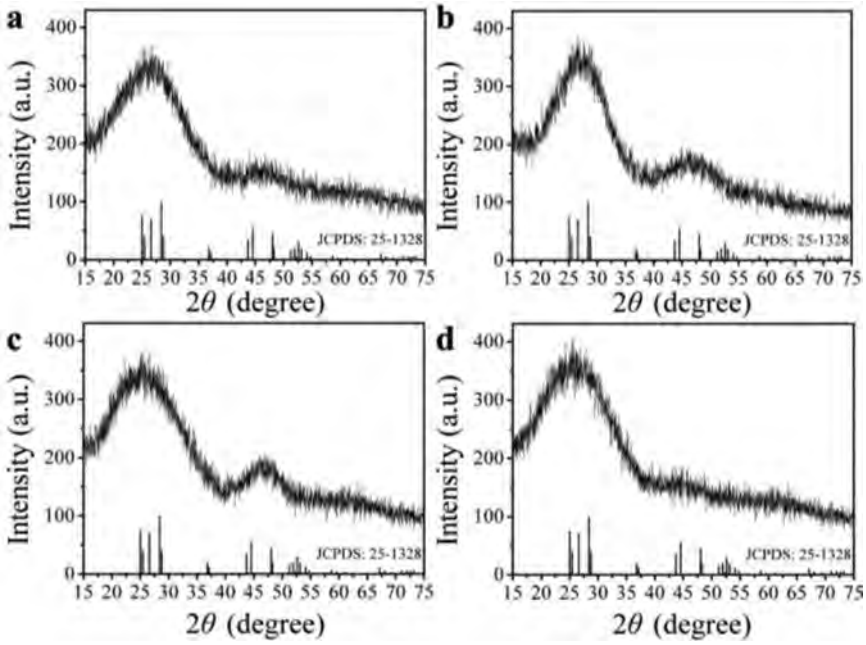

Fig. 5. XRD spectra of $AgInS_2$ QDs synthesized at 50 °C (a) without ripening, and ripened at (b) 30 °C, (c) 50 °C and (d) 70 °C.

4.1 ± 0.6 nm (30 °C, Figs. 4a–c), 4.5 ± 0.7 nm (50 °C, Figs. 4d–f) and 5.0 ± 1.5 nm (70 °C, Figs. 4g–i), with the size homogeneities decreased. The increased particle sizes of QDs ripened at 50 °C and 70 °C rightly corresponded to the red-shifted fluorescence peak positions of the QDs products. And according with the Ostwald ripening model [24], the decreased size homogeneities were due to the constant dissolving of the QDs with smaller size, and the constant growing of the QDs with larger size during the ripening process, which minimized the free energy of the whole system. In addition, it was shown that $AgInS_2$ QDs ripened at 70 °C had the poorest crystallinity (Fig. 4h).

Then, we measured the XRD spectrum of the QDs products synthesized at 50 °C before and after ripened at all set temperatures, to further explore how the ripening temperature affected the crystallinity of the QDs products. The results were shown in Fig. 5. Corresponding to standard cards (JCPDS No. 25-1328), lower ripening temperatures (30 and 50 °C) made the characteristic diffraction peaks (2θ at 43.7°, 44.5° and 48.1°) of QDs sharper than that of QDs without ripening, indicating that the crystallinity of QDs was improved, which might correspond to the increased FI at these ripening temperatures [25]. However, the intensities of the characteristic diffraction peaks of (040)/(320) and (123) phases, corresponding to QDs' 2θ at 44.5° and 48.1°, decreased obviously when QDs were ripened at 70 °C. It indicated that the original crystalline state of QDs might be destroyed in this ripening process, and the crystallinity of QDs became worse, which corresponds with the TEM results. This might be due to the too fast growing of the QDs at such a high ripening temperature, leading to a high lattice mismatch ratio and poor crystallinity, so that the fluorescence intensity of the QDs products decreased [26].

Finally, the QYs of the $AgInS_2$ QDs products synthesized at 50 and 70 °C before and after being ripened at 50 °C and 70 °C were also compared. The QY increased from 3.9% (synthesized at 50 °C) and 8.8% (synthesized at 70 °C) to 9.6% and 10.3% respectively through on-line ripening at 50 °C, while decreased to 3.1% and 3.4% respectively when the ripening temperature reached to 70 °C. And this result corresponds well with our deduction about the ripening process at 70 °C above. Altogether, the characterization analysis above shows that high-temperature ripening process (ripening at 70 °C) changed the original crystal structure of the QDs products, causing the increase of QDs' defects and the decrease of QDs' QY, which consequently decreased the QDs' FI.

In conclusion, we designed an integrated microfluidic chip to screen the most suitable temperature combination in the synthesis and ripening process of water-soluble $AgInS_2$ QDs preparation, to get high-quality QDs products. Taking advantage of the high stability of the droplet microreactors, and the unique space-time-transformation characteristics of the droplet microfluidic chip, successive synthesis-ripening of $AgInS_2$ QDs was conducted in an automated way, with the temperatures regulated independently. It was found that the synthesis and the ripening temperatures affect the fluorescence performance of $AgInS_2$ QDs in a synergistic way. With the synthesis temperature adjusted from 30 °C to 70 °C, the emission peak position of the $AgInS_2$ QDs products red-shifted from 589 nm to 720 nm. However, though the ripening temperature plays a role in the emission peak regulation as important as the synthesis temperature, it is better to set it lower than the synthesis temperature to effectively enhance the FI of the QDs products. Guided by this law, we successfully enhanced the QY of $AgInS_2$ QDs synthesized at 70 °C, from 8.8% [22] to 10.3%, after the ripening at 50 °C.

Declaration of competing interest

The authors declare no conflict of interest.

Acknowledgment

This work was supported by the National Natural Science Foundation of China (Nos. 22074107, 21775111).

Supplementary materials

Supplementary material associated with this article can be found, in the online version, at doi:10.1016/j.cclet.2021.11.022.

References

[1] L. Wang, X.J. Kang, D.C. Pan, Inorg. Chem. 56 (2017) 6122–6130.

[2] J. Li, X.F. Lin, Z.Y. Zhang, W.W. Tu, Z.H. Da, Biosens. Bioelectron. 126 (2019) 332–338.
[3] H.X. Shi, L.C. Jia, C.J. Wang, et al., Opt. Mater. 99 (2020) 109549.
[4] D.L. Su, L. Wang, M. Li, et al., J. Alloys Compd. 824 (2020) 153896.
[5] J. Zhang, B. Zeng, H.H. Ye, A.W. Tang, Chin. Chem. Lett. 32 (2021) 1507–1510.
[6] S. Jain, S. Bharti, G.K. Bhullar, S.K. Tripathi, J. Lumin. 219 (2020) 116912.
[7] A. Delices, D. Moodelly, C. Hurot, et al., ACS Appl. Mater. Interfaces 12 (2020) 44026–44038.
[8] O.S. Oluwafemi, B.M.M. May, S. Parani, J.V. Rajendran, J. Mater. Res. 34 (2019) 4037–4044.
[9] L. Tian, H.I. Elim, W. Ji, J.J. Vittal, Chem. Commun. 41 (2006) 4276–4278.
[10] Y. Liu, X.Y. Jiang, Lab Chip 17 (2017) 3960–3978.
[11] P. Sahu, B.L.V. Prasad, Langmuir 30 (2014) 10143–10150.
[12] Z.S. Campbell, F. Bateni, A.A. Volk, K. Abdel-Latif, M. Abolhasani, Part. Part. Syst. Charact. 37 (2020) 2000256.
[13] L. Frenz, A. El Harrak, M. Pauly, et al., Angew. Chem. Int. Ed. 47 (2008) 6817–6820.
[14] E. Amstad, M. Gopinadhan, C. Holtze, et al., Science 349 (2015) 956–960.
[15] G.D. Niu, A. Ruditskiy, M. Vara, Y.N. Xia, Chem. Soc. Rev. 44 (2015) 5806–5820.
[16] L.L. Lin, Y.J. Yin, S.A. Starostin, et al., Chem. Eng. J. 425 (2021) 131511.
[17] Y.M. Zeng, L.J. Pan, J. Wang, et al., ChemistrySelect 5 (2020) 5889–5894.
[18] Y. Shu, P. Jiang, D.W. Pang, Z.L. Zhang, Nanotechnology 26 (2015) 275701.
[19] L.J. Pan, J.W. Tu, H.T. Ma, et al., Lab Chip 18 (2018) 41–56.
[20] J. Baek, P.M. Allen, M.G. Bawendi, K.F. Jensen, Angew. Chem. Int. Ed. 50 (2011) 627–630.
[21] A. Yashina, I. Lignos, S. Stavrakis, J. Choo, A.J. DeMello, J. Mater. Chem. C 4 (2016) 6401–6408.
[22] H.T. Ma, L.J. Pan, J. Wang, L. Zhang, Z.L. Zhang, Chin. Chem. Lett. 30 (2019) 79–82.
[23] J.R. Shimpi, D.S. Sidhaye, B.L.V. Prasad, Langmuir 33 (2017) 9491–9507.
[24] Y. Yin, A.P. Alivisatos, Nature 437 (2005) 664–670.
[25] D.C. Che, X.X. Zhu, H.Z. Wang, et al., J. Colloid Interface Sci. 463 (2016) 1–7.
[26] W.M. Girma, M.Z. Fahmi, A. Permadi, M.A. Abate, J.Y. Chang, J. Mater. Chem. B 5 (2017) 6193–6216.